JOURNAL OF GEOPHYSICAL RESEARCH, VOL. 115, C04024, doi:10.1029/2009JC005535, 2010

Lagrangian and Eulerian observations of the surface circulation in the Tyrrhenian Sea

E. Rinaldi,[1] B. Buongiorno Nardelli,[1] E. Zambianchi,[2] R. Santoleri,[1] and P.-M. Poulain[3]

Received 26 May 2009; revised 19 October 2009; accepted 12 November 2009; published 28 April 2010.

[1] This paper focuses on the study of the Tyrrhenian Sea, a subbasin of the western Mediterranean whose surface and near-surface dynamics are still relatively poorly known, in particular, its southern region. Its circulation is described first by a set of 53 surface drifters deployed in the area between December 2001 and February 2004. In order to supplement the drifter data with continuously and uniformly sampled observations and to characterize the seasonal, as well as higher-frequency variability of the surface circulation, the Lagrangian analysis was associated to simultaneous satellite remotely sensed altimeter, covering the period 2001–2004. The investigation was based on trajectory analysis and on the computation of the pseudo-Eulerian statistics using the same binning and space-time averaging for drifter and altimeter data. The data reveal a complex pattern of the circulation, especially in the southern region of the Tyrrhenian, dominated by semipermanent recirculations and transient features, which sometimes makes it difficult to identify a consistent mean flow, while the northern subbasin is characterized by a pair composed of cyclonic and anticyclonic circulations known in the literature as the North Tyrrhenian Cyclone and North Tyrrhenian Anticyclone. The pseudo-Eulerian statistics computed with the two data sets evidenced the representativeness of a joint analysis of altimeter and drifter data and yielded useful indications about proper preliminary preprocessing and resampling procedures, so as to make the comparison statistically sound.

Citation: Rinaldi, E., B. Buongiorno Nardelli, E. Zambianchi, R. Santoleri, and P.-M. Poulain (2010), Lagrangian and Eulerian observations of the surface circulation in the Tyrrhenian Sea, *J. Geophys. Res.*, *115*, C04024, doi:10.1029/2009JC005535.

1. Introduction

[2] Although the main characteristics of the Mediterranean Sea are well known [*Malanotte-Rizzoli et al.*, 1999; *Robinson et al.*, 2001], our knowledge of the processes taking place in one of its subbasins, the Tyrrhenian Sea (Figure 1), is not yet fully exhaustive. The aim of this paper is to analyze recently available data to characterize the Tyrrhenian Sea surface circulation and its variability especially in the southern region of the basin, which is by far the least well known.

[3] The Tyrrhenian Sea is one of the major subbasins of the Mediterranean. It has a triangular shape and a very complex bathymetry and is connected to the outer Mediterranean Sea with the Corsica Channel (north) and a broad opening to the southwest, between Sardinia and Sicily. This basin plays an important role in the transformation of the main Mediterranean intermediate and deep waters [*Astraldi and Gasparini*, 1994; *Gasparini et al.*, 1999; *Sparnocchia et al.*, 1999] occasionally resulting in the formation of Tyrrhenian dense water [*Astraldi and Gasparini*, 1994].

[4] Even though the first investigations on the Tyrrhenian date from hundred years ago [*Nielsen*, 1912] and the basin was the object of a thorough investigation carried out in the framework of the International Geophysical Year [*Aliverti et al.*, 1968], direct measurements of velocities and transports in the Tyrrhenian Sea are still very sparse. Available information are mainly based, on one hand, on the in situ measurements collected in the north part of the basin during "TEMPO" surveys in the late 1980s/early 1990s [*Astraldi and Gasparini*, 1994; *Marullo et al.*, 1994] and by the limited data collected at its southern entrance by *Sparnocchia et al.* [1999].

[5] These data allowed a satisfactory hydrological characterization of the Tyrrhenian Sea, even though the mechanisms of observed long-term changes still have to be fully understood. On the other hand, the informations on the circulation in the basin, especially at the surface, are much less accurate. The traditional concept [*Millot*, 1987, 1999] of a cyclonic circulation at all levels appears to be far too schematic: recent Eulerian (for the deep layer, see P. Falco (personal communication on unpublished data, 2009)) and Lagrangian studies (we refer in particular to the MedArgo data regarding

[1]Istituto di Scienze dell'Atmosfera e del Clima, CNR, Rome, Italy.
[2]Dipartimento di Scienze per l'Ambiente, Università degli Studi di Napoli "Parthenope," Naples, Italy.
[3]Dipartimento di Oceanografia, Istituto Nazionale di Oceanografia e di Geofisica Sperimentale, Trieste, Italy.

0148-0227/10/2009JC005535

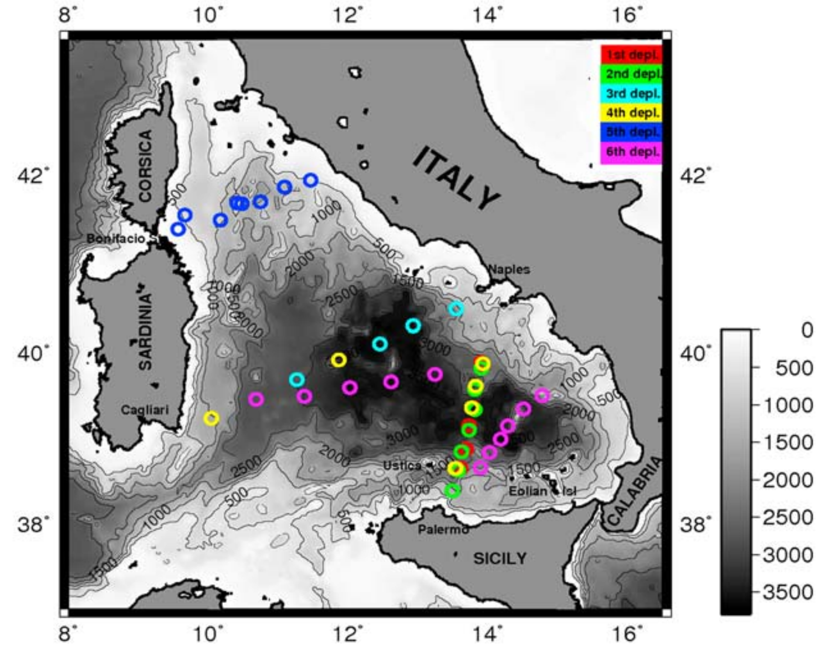

Figure 1. Map of the Tyrrhenian Sea with its bathymetry and the different drifter deployment locations (see also Table 1 for information on the individual deployments).

the intermediate water circulation [*Poulain et al.*, 2007]) show a remarkable and unexpected complexity.

[6] In the past, efforts have been concentrated on some elements of the surface dynamics of the northern portion of the basin where TEMPO data were available, whereas the southern part has not been practically explored. The northwest Tyrrhenian is dominated by the presence of an important feature, the North Tyrrhenian Cyclone (NTC [see *Marullo et al.*, 1994]), induced by strong northwesterly winds channeled by the Strait of Bonifacio, presenting a strong seasonal variability and affecting the coastal currents flowing along the northeastern flank of the basin. Past observations show that this northern gyre, whose dimensions are of the order of 100 km, displays a strong seasonal dependence in size and position. During winter it is stretched along the meridional direction in the western part of the basin, while in summer it is zonally oriented [*Artale et al.*, 1994; *Astraldi and Gasparini*, 1994] capturing a weak flow along the Italian Peninsula. In summer, both cyclonic and anticyclonic eddies with characteristic length scales of 30–40 km are nested within the larger gyre [*Artale et al.*, 1994]. *Marullo et al.* [1994], on the basis of AVHRR thermal images analysis, suggested that the NTC in summer consists of a cold water filament originating from the Strait of Bonifacio and extending eastward, rather than being a well organized cyclonic structure. Despite this different interpretation of the NTC structure past studies agree that the change of NTC orientation (zonal/meridional in summer/winter) is due to the strengthening of the current that drives the circulation through the Corsica Channel.

[7] South of the NTC, an anticyclonic gyre (North Tyrrhenian Anticyclone (NTA)) is present. The generation and evolution of these gyres is also controlled by the strong wind events affecting the Strait of Bonifacio, and specifically by the wind stress curl associated with the easterly winds, and its associated Ekman pumping [*Crépon et al.*, 1989; *Artale et al.*, 1994].

[8] The seasonal variability of the northern Tyrrhenian is also mirrored in the water exchange between the Tyrrhenian and the Ligurian Sea, mainly driven by steric effects, which dominate in the winter season [*Astraldi and Gasparini*, 1994; *Marullo et al.*, 1994; *Vignudelli et al.*, 1999, 2000], with an interannual variability possibly linked with regional teleconnection phenomena, namely the North Atlantic Oscillation [*Vignudelli et al.*, 1999].

[9] In the southern part of the basin, the dynamics are conditioned by the exchanges through the straits of Sicily and Sardinia. Surface water of Atlantic origin (AW) enters the Tyrrhenian Sea off the northern Sicilian coast [see, e.g., *Krivosheya and Ovchinnikov*, 1973]. It is believed to flow eastward along the northern coast of Sicily, following an overall cyclonic pattern, proceeding along the western coast of Italy and then entering the Ligurian Sea through the Corsica Channel [*Aliverti et al.*, 1968; *Elliot and De Strobel*, 1978; *Tait*, 1984].

[10] Using Lagrangian data collected in the Straits of Sicily in the 1990s, *Poulain and Zambianchi* [2007] recently showed that waters coming from the Algerian Current indeed flow northeastward into the Tyrrhenian, along the Sicilian coast. Their analyses clearly indicated that this flow returns southbound on the western side of the Sardinian Channel and forms a rather stable cyclonic gyre.

[11] It is clear that the variability of the main features modulating the Tyrrhenian large-scale current system still needs investigation and little is known, for example, about the energy involved in mesoscale processes. As a consequence, in this paper we try to fill this particular gap through the analysis of satellite altimeter measurements and Lagrangian surface data.

Table 1. Deployment and Lifetime of Drifters Analyzed in This Study

Deployment	Drifter Number	Deployment Date	Last Transmission
1	33198	14 Dec 2001	2 Jun 2002
1	33199	14 Dec 2001	24 Jan 2002
1	33202	14 Dec 2001	2 Apr 2002
1	33203	14 Dec 2001	31 Dec 2001
1	33204	14 Dec 2001	21 May 2002
1	33252	14 Dec 2001	5 Mar 2002
1	33253	14 Dec 2001	25 Feb 2002
1	33254	14 Dec 2001	2 Feb 2002
2	33207	27 Jun 2002	2 Jul 2002
2	33208	27 Jun 2002	16 Nov 2002
2	33210	27 Jun 2002	29 Aug 2002
2	33211	27 Jun 2002	30 Jul 2002
2	33212	27 Jun 2002	19 Jul 2002
2	33213	27 Jun 2002	29 Jul 2002
2	33214	27 Jun 2002	6 Sep 2002
2	33249	27 Jun 2002	11 Jul 2002
2	33250	27 Jun 2002	10 Jul 2002
2	33251	27 Jun 2002	11 Jul 2002
3	33215	3 Oct 2002	15 Jan 2003
3	33216	3 Oct 2002	21 Apr 2003
3	33217	4 Oct 2002	4 Nov 2002
3	33218	4 Oct 2002	14 Oct 2002
3	33219	4 Oct 2002	21 Jan 2003
4	33222	28 Jan 2003	5 Apr 2003
4	33223	28 Jan 2003	22 Jul 2003
4	33224	28 Jan 2003	8 May 2003
4	33231	31 Jan 2003	5 Sep 2003
4	33235	31 Jan 2003	3 Feb 2003
4	33236	31 Jan 2003	22 Jul 2003
4	33246	28 Jan 2003	8 Jul 2003
4	33247	28 Jan 2003	1 Feb 2003
4	33248	28 Jan 2003	27 Apr 2003
5	34447	17 Apr 2003	27 Oct 2003
5	34448	17 Apr 2003	18 Oct 2003
5	34449	20 Apr 2003	16 May 2003
5	34450	17 Apr 2003	1 Jul 2003
5	39428	17 Apr 2003	8 Sep 2003
5	39429	17 Apr 2003	2 Nov 2003
5	39430	17 Apr 2003	17 Aug 2003
5	39431	17 Apr 2003	20 Sep 2003
6	39432	9 Aug 2003	19 Feb 2004
6	39433	10 Aug 2003	2 Oct 2003
6	39434	9 Aug 2003	8 Dec 2003
6	39435	9 Aug 2003	27 Feb 2004
6	39436	9 Aug 2003	4 Feb 2004
6	39437	10 Aug 2003	9 Oct 2003
6	39438	9 Aug 2003	24 Oct 2003
6	39440	8 Aug 2003	12 Aug 2003
6	39441	10 Aug 2003	15 Oct 2003
6	39442	8 Aug 2003	7 Sep 2003
6	39443	9 Aug 2003	28 Sep 2003
6	39444	8 Aug 2003	12 Dec 2003
6	39445	8 Aug 2003	31 Aug 2003

[12] On one hand, satellite data can provide long-term, synoptic, and global estimates of key parameters of the oceans, but they still need to be validated by available in situ measurements. On the other hand, dynamical structures with very fast propagation velocities or short life duration cannot be studied by means of altimeter data that can only monitor processes at temporal scales longer than ~10 days. On the contrary, Lagrangian data provide information on short-term variability of the surface field but can be intermittent in space/time due to the limited number of drifters available.

[13] While both Lagrangian and altimeter data have been extensively used in the past to study the Mediterranean ocean surface circulation separately [e.g., *Larnicol et al.*, 2002; *Iudicone et al.*, 1998; *Buongiorno Nardelli et al.*, 2002; *Pujol and Larnicol*, 2005; *Poulain and Zambianchi*, 2007], here more than three years of Lagrangian data acquired in the Tyrrhenian Sea from 2001 to 2004 are presented and analyzed together with coincident altimeter data. Trajectory analysis and different kinds of pseudo-Eulerian statistics applied to the Lagrangian and to satellite data are thus analyzed to identify the mean patterns of the Tyrrhenian Sea circulation as well as the variability of its basin, subbasin and mesoscale structures. To our knowledge, the method chosen here, namely comparing filtered drifters statistics with resampled altimeter data over drifters trajectories (see section 4) represents an innovative approach that served to complement and compare the information provided by two data sets separately and helped to quantify the impact of the different sampling strategy of the two instruments, as well as the dynamical limitations of altimeter derived velocities in representing the ocean surface circulation.

2. Data

2.1. Drifting Buoy Data Set

[14] The in situ data used in this study were obtained from 53 satellite-tracked modified CODE drifters deployed in the Tyrrhenian Sea and contributing data from December 2001 to February 2004. This Lagrangian experiment was organized in the framework of the "Programma Ambiente Mediterraneo" initiative, funded by the Italian Ministry for Research, with additional funding obtained from the U.S. Office of Naval Research.

[15] The modified CODE drifters have the same structure of the original ones, conceived for and used in the Coastal Dynamics Experiment (CODE) in the early 1980s [*Davis*, 1985]. They consist of a vertical, 1 m long plastic tube, containing the electronics and the transmission package and antenna, with four sails extending radially from the tube over its entire length, which maximize the surface current drag. The total vertical extent of the system is about 1 m. The buoyancy is provided by four small floating spheres tethered to the upper and outer extremities of the sails.

[16] Comparison with current meter measurements [*Davis*, 1985] and surface ocean dye experiments (D. Olson, personal communication, 1991) show that velocities estimated from CODE drifter trajectories are accurate to about 3 cm/s, even under strong wind conditions.

[17] All drifters were tracked by the Argos Data Collection and Location System.

[18] In order to explore the most efficient transmission duty cycle in terms of cost-effectiveness and at the same time accuracy of velocity derivation, various transmission duty cycles were tried for this study. The raw drifter data were first edited for spikes and outliers [*Poulain et al.*, 2004]. They were then interpolated at 2 hour intervals using a kriging technique, and low-pass filtered (36 hour cut-off) to remove high-frequency current components. Finally, the low-pass time series were subsampled every 6 hours and the surface velocities have been estimated through centered finite differencing of the filtered positions.

[19] The Tyrrhenian Lagrangian experiment consisted of six successive deployment episodes. Deployment time and location as well as drifter lifetimes are summarized in Table 1, and deployment locations are also shown in Figure 1. Drifter

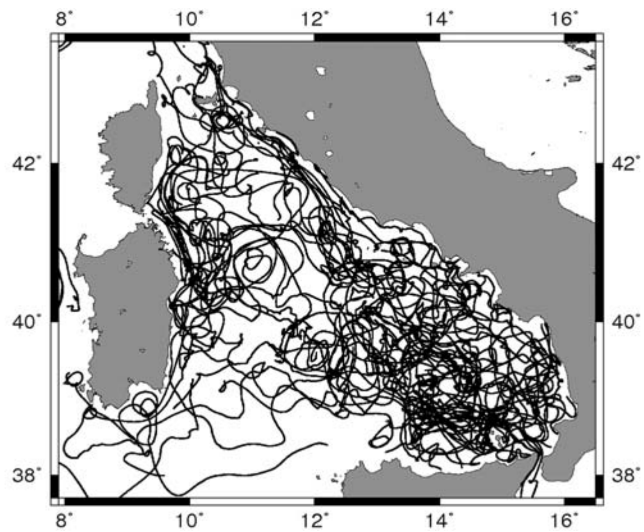

Figure 2. Composite of all trajectories of drifters deployed in Tyrrhenian Sea from 2001 to 2004 analyzed in this study.

deployments had been originally planned so as to take advantage of the Tyrrhenian coastal current, allegedly a swift current flowing along the western coast of the Italian Peninsula from the extreme South (Calabria) all the way northeastward to the Corsica Channel. Therefore most of the drifters have been launched in the southeastern region of the Tyrrhenian.

[20] The total number of observation days gathered in this experiment is around 5000 drifter days, and the average lifetime of drifters amounts to 90 days approximately (Table 1). In Figure 2 we show the spaghetti diagram of all drifter trajectories and in Figure 3 the relative drifter data density (in 0.5° × 0.5° bins) in the Tyrrhenian. The absolute maximum of data density is located in the southeastern portion of the basin. This is partly due to the deployment locations, and mostly to the circulation in that area, which yields a longer renewal time for surface water there rather than in other subbasins. Another (relative) density maximum is displayed in correspondence to the southward current flowing along the Sardinian coasts, and a further, very weak maximum in the area south of the Corsica Channel.

[21] Pseudo-Eulerian statistics have been computed from this data set (for the definitions of mean kinetic energy MKE, eddy kinetic energy EKE and of the variance ellipses see *Emery and Thomson* [1998] and *Poulain and Zambianchi* [2007]). The pseudo-Eulerian approach is a classical tool utilized in the study of Lagrangian data and consist of subdividing the domain under observation into regions (bins) within which the flow is assumed to be homogeneous and stationary, and by computing the mean field as the average of all the velocity measurements available in the bin [*Swenson and Niiler*, 1996; *Poulain*, 2001] (for a thorough methodological discussion see *Bauer et al.* [1998]). The bin size has to be selected so as to contain a large number of measurements to ensure robustness of the inferred statistical quantities; at the same time bins have been kept small enough to achieve an appropriate space resolution, and to avoid an excessive smoothing of the mean field and the consequent erroneous inclusion of a portion of it in the residuals. In this study bins of 0.25° × 0.25° are used.

2.2. Wind Data

[22] In order to evaluate the Ekman component from the velocity field deduced by drifters, we have used the operational analysis of wind data provided by the European Centre for Medium-range Weather Forecast (ECMWF) for the period relative to the drifter measurements.

[23] The ECMWF wind data are relative to a height of 10 m above the sea surface and have a spatial resolution of 0.5° × 0.5° and temporal resolution of 6 hours. Wind-driven currents estimated from wind data on the basis of Ekman's theory have been evaluated using drifter data by several authors (see, e.g., the recent examples by *Ralph and Niiler* [1999] and *Rio and Hernandez* [2004] and the application to the eastern Mediterranean by *Poulain et al.* [2009], which summarizes earlier efforts on this issue). Here we have used the general formula for the Mediterranean proposed by *Mauri and Poulain* [2004]

$$Uwind - driven = 0.012\ \exp(-i24^\circ)\,Uwind.$$

[24] The wind data have been interpolated at the time of observation and at the drifter positions using a bilinear scheme. The Ekman component has then been removed from drifter velocities, and the resulting Ekman-corrected drifter observations have undergone the same binning above described for the original drifter data.

2.3. Altimeter Data Set

[25] The altimeter data considered are the updated Mediterranean Absolute Dynamic Topography (MADT) maps from four altimetric satellites Jason-1, Envisat or ERS-2, Topex/Poseidon and Geosat Follow-On GFO, (TOPEX/POSEIDON was substituted by Jason since June 2002, and ERS2 by ENVISAT since July 2003), covering the period of the Tyrrhenian Lagrangian experiment (from January 2001

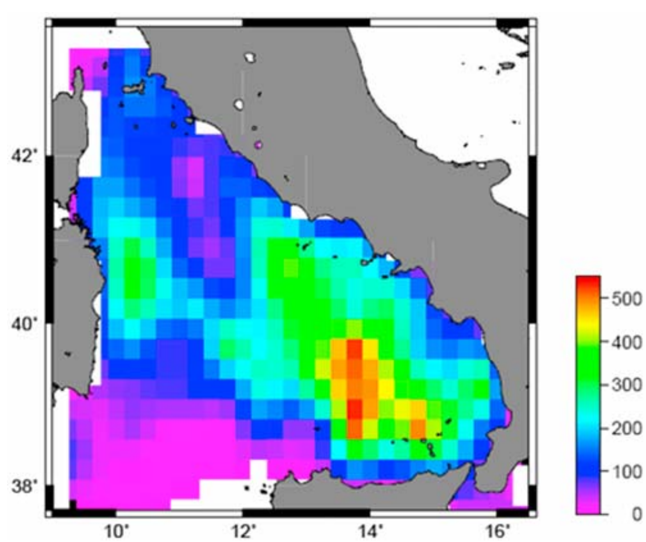

Figure 3. Drifter data density in 6 hourly data points.

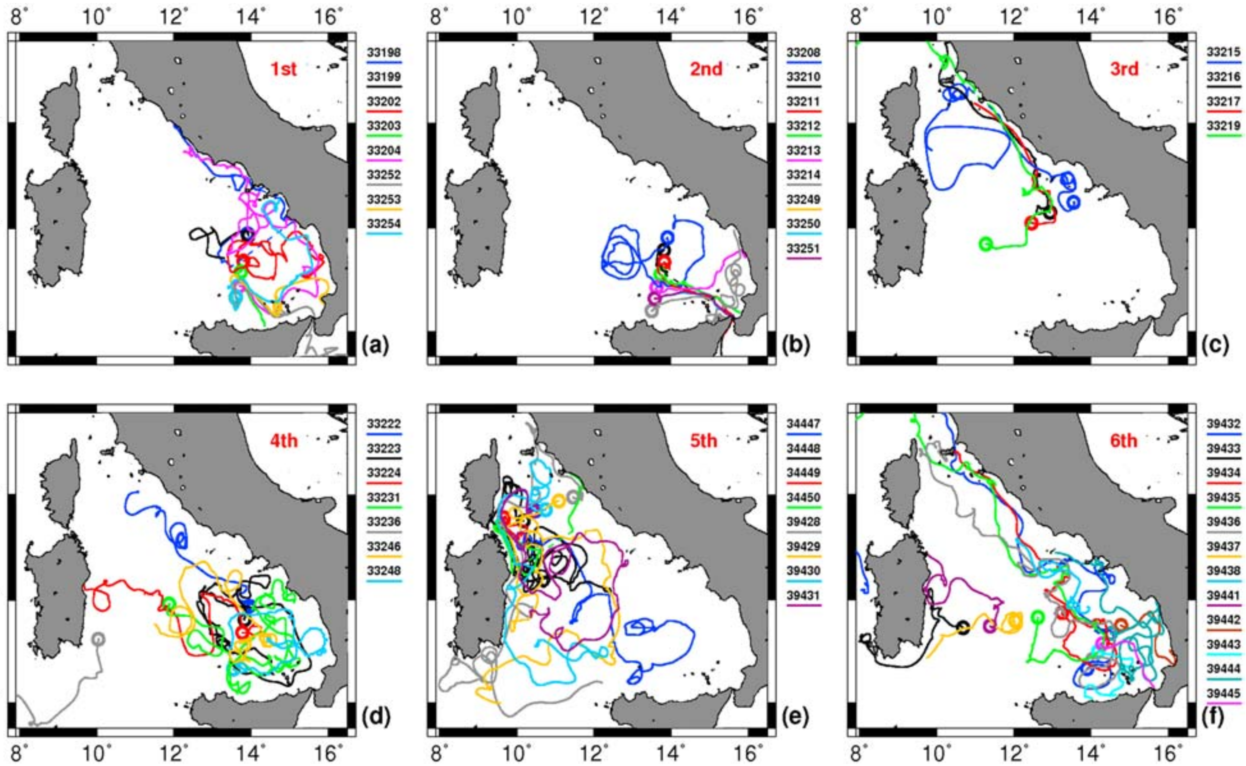

Figure 4. Drifter trajectories for the different deployments: (a) 1st, (b) 2nd, (c) 3rd, (d) 4th, (e) 5th, and (f) 6th deployments (see also Table 1 for information on the individual deployments; here we show only trajectories longer than 10 days).

to December 2004). The altimeter products were produced by Ssalto/Duacs and distributed by *Aviso*, with support from *Cnes* (http://www.aviso.oceanobs.com/duacs/).

[26] These altimeter data are interpolated by AVISO over a regular 1/8° grid on a weekly basis, using an optimal interpolation method that merges the data coming from the diverse altimeter missions, directly adjusting the residual long-wavelength errors [*Ducet et al.*, 2000]. The covariance function used by this interpolation procedure is shaped as:

$$C(r,t) = \left[1 + ar + \frac{1}{6}(ar)^2 - \frac{1}{6}(ar)^3\right] e^{-ar} e^{\left(\frac{t}{T}\right)^2},$$

where the parameters a and T practically lead to space and time decorrelation scales of about 100 km and 10 days, respectively.

[27] Finally, the Absolute Dynamic Topography is computed adding a mean dynamic topography (MDT) to the sea level anomalies (SLA). The method applied to calculate the MDT was developed and described by *Rio and Hernandez* [2004] and has been specifically applied to the Mediterranean data by *Rio et al.* [2007].

[28] From the MADT, we estimate the surface velocities assuming the geostrophic approximation, which enables to obtain the surface velocity from the gradients of the ocean topography. In order to be consistent with the procedure used for drifter data, we applied the pseudo-Eulerian approach also to altimeter data, so that the altimeter geostrophic velocities were first binned over the same 0.25° × 0.25° grid used for Lagrangian data and then used to compute the statistics.

3. Analysis of the Surface Circulation

3.1. Surface Circulation Revealed by Drifters Trajectories

[29] The general picture of the surface circulation coming out of the drifter trajectories can be outlined as follows (see Figures 2 and 4): once the surface waters penetrate into the Tyrrhenian, they typically undergo a northward deflection in correspondence to complex bathymetric features of the Sicilian shelf break (Figure 4e). Rather than continuing cyclonically along the Sicilian and then along the Italian continental coastline, the core of the surface transport off north-west Sicily is thus displaced offshore. The shelf area next to the Sicilian coast west of the Eolian Islands is characterized by recirculations rather than by the expected eastward zonal flow (see Figures 4a, 4d, and 4f). In particular, the trajectories show the presence of a southern anticyclonic recirculation and of a northern cyclonic one, connected to the coastal flow further north (Figures 4d and 4f), whose presence had been suggested in the geostrophic flow computations by *Krivosheya and Ovchinnikov* [1973], but never substantiated by current data.

[30] The coastal current in the eastern zone of the Tyrrhenian results quite unstable in its southernmost portion, and often branches westward, originating a complex flow

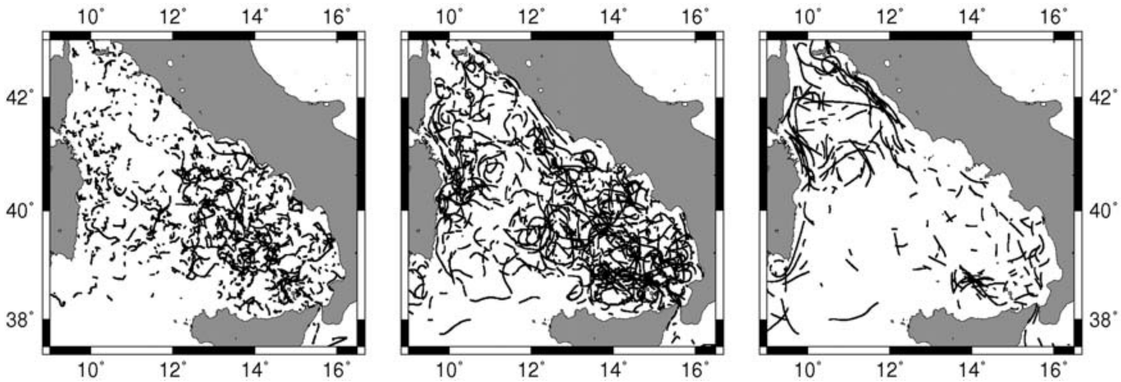

Figure 5. Segments of trajectories corresponding to different drifter speed ranges: (left) lower than 15 cm/s, (middle) between 15 and 25 cm/s, and (right) higher than 25 cm/s.

pattern in the south-central Tyrrhenian basin. Moreover, this current is characterized by recirculations with scales ranging from 20 to 100 km and more, some of which are transient and some of which turn out to be quasi-permanent features of the velocity field (Figure 4d). In particular, the drifter data show the presence of a strong and recurrent anticyclonic circulation in the center of the Southern Tyrrhenian very well caught by drifters 33204 and 34447 (Figure 4b). We will refer to it, in analogy with the above mentioned NTA and NTC, as South Tyrrhenian Anticyclone (STA), which is further investigated in the following with the aid of altimeter data. The eastern coastal current becomes a steady and recurrent feature of the surface Tyrrhenian circulation only north of the Gulf of Naples (Figures 2, 4a, 4c, and 4d). From there on, it flows close to the coast all the way to the Corsica Channel, occasionally changing direction with local recirculations which bring its waters into marginal subbasins (bays and gulfs) or into the offshore regions (Figure 4). We have to point out that the drifter trajectories make it through the Corsica Channel into the Ligurian Sea only in winter in agreement with the increase of the Corsica Chanel outflow observed by currentometer records collected in that area [*Vignudelli et al.*, 1999, 2000]. This indicates that the northward coastal flow undergoes seasonal variability. In the northern Tyrrhenian, the return circulation is ensured by the NTC and by its southern counterpart, the NTA, which also in our data show some degree of seasonal variability, possibly contributing to the variability of the throughflow across the Corsica Channel (Figures 4c and 4e).

[31] After tracing the two vortices, the southward flow closing the broad cyclonic circulation in the direction of the Sardinia Channel also "leaks" into the basin, nourishing several recirculations (Figure 4e). Given all the above, the flow in the interior of the basin is dominated by transient and only occasionally quasi-steady vortices, and, despite the vicinity to the Sardinia Channel, it is very difficult to identify a mean flow pattern in the southern section of the Tyrrhenian (Figure 2), as mirrored in the pseudo-Eulerian statistics (see below).

[32] The separation of the Tyrrhenian circulation in two regimes is clearly shown in the portions of trajectories plotted according to the drifter speed (Figure 5). Figure 5 nicely displays the deductions drawn from the trajectory analysis: the slowest speeds (less than 15 cm/s) dominate the central-southern area of the basin; speeds between 15 and 25 cm/s are clearly associated with mesoscale and subbasin recirculation structures, and are ubiquitous in the whole Tyrrhenian; fastest speeds are associated with the (northern) Tyrrhenian coastal current, as we would like to define it from now on, with the Corsican-Sardinian coastal current, i.e., the southward coastal current flowing along the western boundary of the basin, and also limited to the northern part of it, and occasionally with the jet-like flow of AW directed between Ustica and the Eolian Islands.

[33] Given the limited number of instruments available for this experiment, it is not possible to adequately describe the exchange between the Tyrrhenian and the neighboring basins. As to the northward outflow of surface Tyrrhenian water through the Corsica Channel, it is worth noticing, however, that only four out of ten drifters approaching the channel flowed through it into the Ligurian Sea. The outflow described by these four drifters occurred between mid-November and mid-December of two different years, confirming the seasonal character of the flow in that area, possibly driven by the steric difference between Tyrrhenian and Ligurian Sea level [*Vignudelli et al.*, 2000].

[34] On the opposite side of the basin, various drifters deployed in the Southern Tyrrhenian were stranded in the close vicinity of the Strait of Messina, or even crossed it and entered the Ionian Sea. This happened in three out of four southern deployments, and in particular to one over eight drifters deployed during the 1st deployment episode, five over nine in the 2nd, one over nine in the last one.

[35] Three out of the seven drifters approaching the Strait of Messina eventually crossed it and made it into the Ionian Sea. This pathway from the Tyrrhenian to the Ionian Sea was also recently inferred in transmitter-equipped Caretta caretta turtle trajectories [*Bentivegna et al.*, 2007]. The drifter data for the first time made a direct observation of this flow.

3.2. Pseudo-Eulerian Analysis of Drifter Data

[36] In Figure 6 we show the maps of pseudo-Eulerian statistics relative to the drifter data which will be compared in section 4 with analogous quantities drawn from altimeter data. The maps of MKE and the mean flow (Figure 6a) well

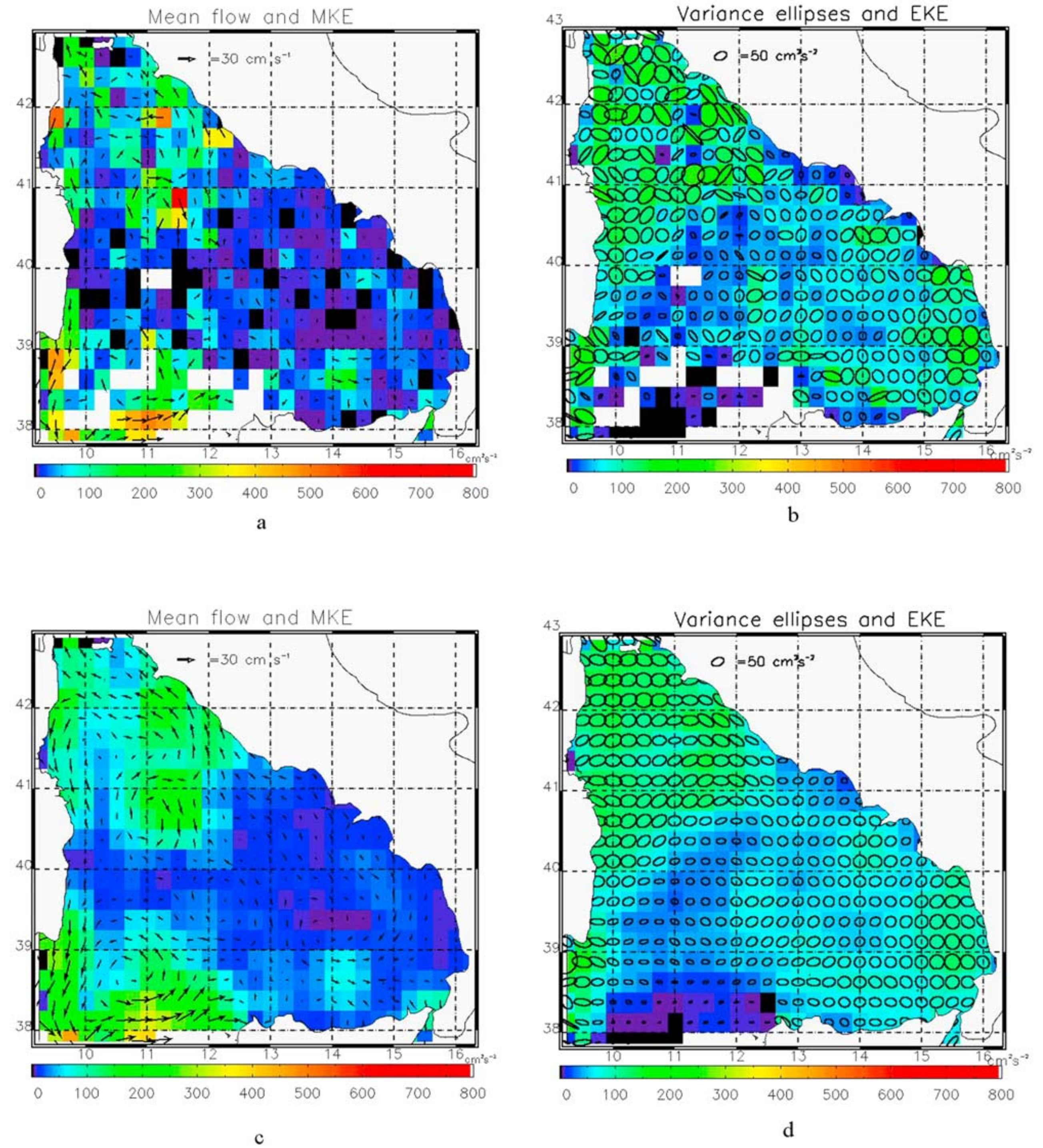

Figure 6. Pseudo-Eulerian statistics from drifter data. (a) Mean kinetic energy with superimposed the mean flow vectors. (b) Eddy kinetic energy with superimposed the variance ellipses. (c) MKE and mean flow vectors obtained smoothing fields shown in Figure 6a. (d) EKE and variances ellipses obtained smoothing fields shown in Figure 6b.

reproduce the general pattern of the circulation described in section 3.1.1. The highest levels of MKE are observed in correspondence to the cyclonic subbasin circulation between Sardinia and Sicily and in the northern regions of the basin in correspondence of the NTC and in the NTA. Moreover the value of some bins in the Corsica Channel (levels of energy greater than 200 cm^2/s^2 and speeds above 20 cm/s) reveal the energetic character of the seasonal flow in this area. In the southeastern region of the Tyrrhenian Sea, it is not possible to identify a clear mean flow, the highest values of MKE being found near the Eolian Islands.

[37] Similarly to what was found for the MKE, high values of EKE (Figure 6b) prevail in the northern part of the basin, where the variance ellipses show a large degree of anisotropy in correspondence of the northern Tyrrhenian coastal current and on the edges of the two main structures, NTC and NTA. A very high variability is also displayed in the southeastern region of the basin, which is particularly remarkable since MKE values in that area are low, thus leading to a strong increase of the EKE/MKE ratio. In this section of the basin the EKE map displays a circular area, between 12 and 16°E 38–40.5°N, with values greater than 150 cm^2/s^2 along the edges of the structure and lower values at its center. Probably, this distribution is due to the variability of STA, of the current flowing off the northern coast of Sicily and of the cyclonic and anticyclonic recirculations west of Eolian Islands.

3.3. Overview of the Surface Circulation as Described by the Altimeter Data

[38] This section describes the surface circulation traced by the altimeter data (Figures 7a and 7b). In the mean field, the NTC anticlockwise rotation emerges as the prominent structure of the circulation in the northern region of Tyrrhenian Sea. The eastern boundary of this gyre is represented by the coastal current leaving the Tyrrhenian Sea through the Corsica Channel. The NTA acts as the southern boundary of the NTC, but it is distinguished by lower values of energy than the NTC. The westward flow of the NTA meets a double core cyclonic gyre that extends as far south as 38°N capturing the major portion of the AW entering the basin. The presence of this gyre can explain the outflow in the western side of the Sardinia Channel observed in hydrological measurements [*Sparnocchia et al.*, 1999; *Astraldi et al.*, 2002]. The highest values of MKE (>135 cm^2/s^2) for this feature are associated with the southward flow along the Sardinian coast and with the southern area of this vortex (MKE > 300 cm^2/s^2). A minor portion of the AW is captured by the STA, the anticyclonic vortex between 12 and 13 E and 39–40 N, having a circular shape with a diameter of ~100 km and MKE level of around 70 cm^2/s^2. An anticyclonic circulation prevails near the northern coast of Sicily, and higher energy is observed in its eastern zone where it encounters another gyre having a cyclonic rotation that extends until 40°N. Offshore the Gulf of Naples, a second anticyclonic recirculation is present. The presence of this series of eddies means that the AW entering in the Tyrrhenian Sea in the eastern part of the Sardinia Channel, rather than flowing cyclonically along the Sicilian and Italian coasts is shifted offshore, creating a more complex surface circulation in the whole southeastern domain of the basin. Qualitatively, the EKE map shows a distribution similar to that of the MKE, with maxima in correspondence of the divergence zone of the NTC and NTA (EKE > 135 cm^2/s^2), along 38°N and along the eastern side of the cyclonic gyre in front of the Calabrian coast (between 15°–16°E and 38°–40°N) where the eccentricity of variance ellipses shows that the variability of the mean flow is prevalently oriented along the northwest-southeast direction. The central area of the Tyrrhenian Sea is characterized by low values of EKE except for the area occupied by the STA. Over the whole basin, the MKE is generally higher than the EKE.

4. Joint Pseudo-Eulerian Analysis of Altimeter and Drifter Data

[39] Even if altimeter measurements are by definition Eulerian and consequently Eulerian statistics might be easily computed from them, in the present analysis the same kind of averaging and binning procedures have been performed on both altimeter and drifter data (thus we will call both pseudo-Eulerian in the following). This choice was driven by the necessity to evaluate the limits and representativeness of both data sets in terms of dynamical and/or sampling factors. In fact, original altimeter data are collected along tracks that are located several kilometers apart, with an instantaneous field of view of ~9 km, and a repetitivity ranging between 10 and 35 days. These data are then used to obtaine interpolated fields, as described in section 2.3. On the opposite, drifter data are characterized by a purely Lagrangian sampling, with large data gaps both in space and time. However, they also provide different measurements of the surface circulation in terms of dynamical components, for example including or not the ageostrophic components of the flow.

[40] The maps of MKE and the mean flow estimated from drifter data and from altimeter are shown in Figures 6a and 7a, respectively. Despite the fact that the general pattern of the circulation shown in the two maps is quite similar, the energy levels are rather different. In general the value of MKE is slightly greater for the altimeter data than for drifters (basin averages are 99 cm^2/s^2 and 74 cm^2/s^2, respectively). In the southeastern area of the basin, the MKE levels appear higher when estimated from the altimeter than from drifter data but the contrary occurs in the western region in correspondence of the NTA and in the western side of NTC.

[41] On the other hand, the two EKE maps (presented in Figures 6b and 7b) are quite different both in terms of structure and orientation of the variance ellipses and in terms of energy values. Energy levels computed from the altimeter are lower than those obtained from drifters almost everywhere (except in the region of divergence of NTC and NTA, 11°E–41°N where the EKE levels of the two maps appear quite comparable). Indeed the average EKE of drifters is 73 cm^2/s^2 while the average EKE of altimeter is 67 cm^2/s^2.

[42] A possible source of the observed discrepancy might be represented by the fact that the altimeter-based dynamic topography actually leaves out the scales of variability that are significantly smaller than the decorrelation length (~100 km) used by the optimal interpolation algorithm.

[43] Moreover, the differences are possibly due to the fact that, despite the 36 hour trajectory filtering removes part of the ageostrophic components of the current, the drifter velocities still contain an ageostrophic component due to the wind-driven Ekman transport, to cyclostrophic balance and/or to rapidly evolving mesoscale features. These components cannot be detected by altimetry, given that the geostrophic approximation has to be assumed in order to estimate velocities from measured surface elevation (see section 2). For that reason, as part of our analysis, the Ekman component has been estimated from the ECMWF wind data and subtracted from the drifter velocities.

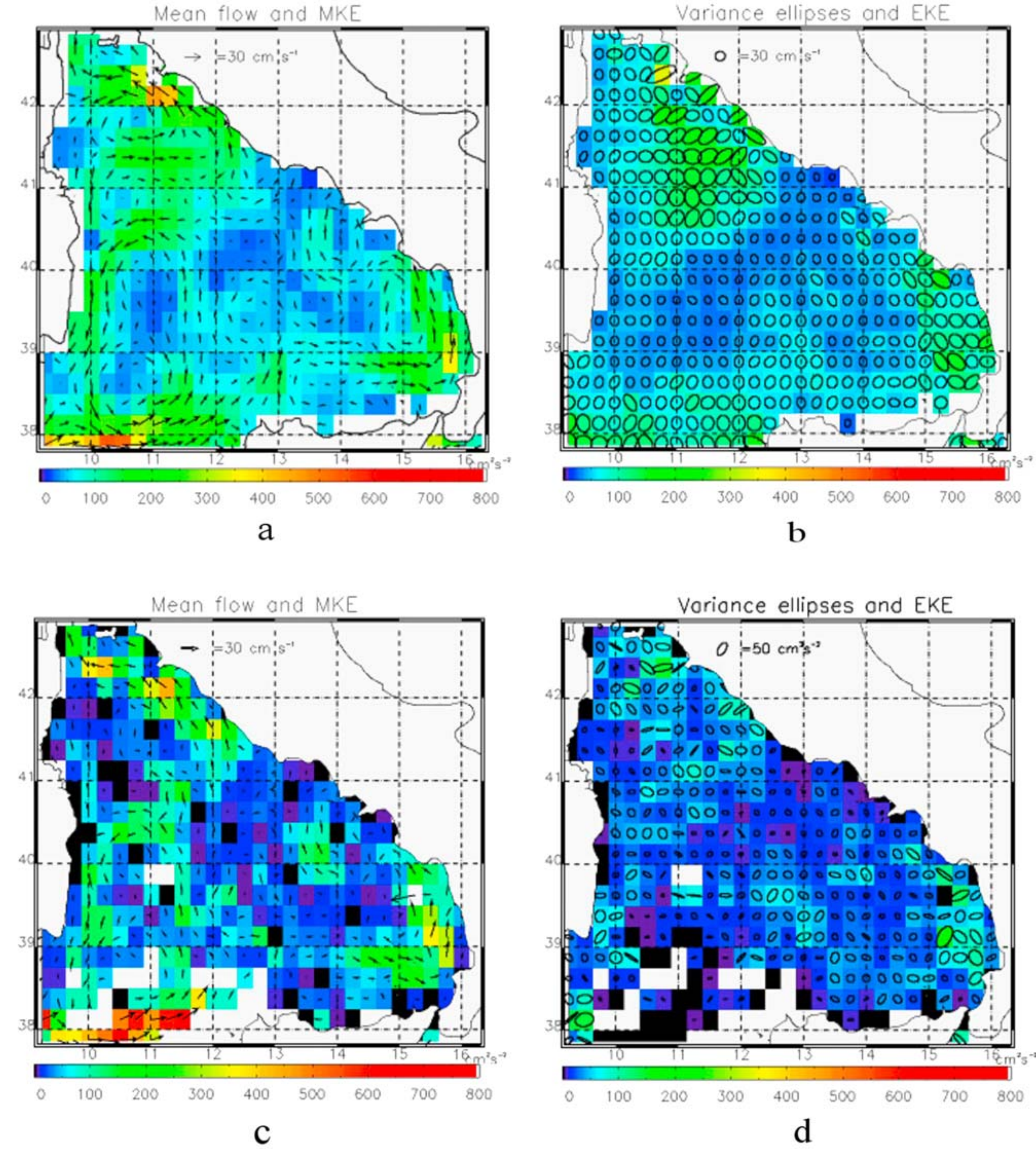

Figure 7. Pseudo-Eulerian statistics from altimeter data. (a) Mean kinetic energy with superimposed the mean flow vectors. (b) Eddy kinetic energy with superimposed the variance ellipses. (c) MKE and mean flow vectors computed using altimeter data sampled in correspondence of the drifter measurements. (d) EKE and variances ellipses computed using altimeter data sampled in correspondence of the drifter measurements.

[44] However, the MKE and EKE statistics calculated from corrected velocities (not shown) do not show large differences from a qualitative standpoint, with respect to those computed from uncorrected data: the mean flow pattern, the eccentricity of variance ellipses as well as the general distribution of MKE and EKE are very similar. The impact of the Ekman correction is of the order of 20% on the EKE (in agreement with the order of magnitude discussed by

Mauri and Poulain [2004]; see also *Poulain et al.* [2009]) and twice as much on the MKE. The corrected trajectories have thus been used hereafter.

[45] The latter value, however, is not surprising, as the mean circulation is not directly related to the instantaneous or short-term wind forcing [see *Mauri and Poulain*, 2004]. This is the case of the NTC and the NTA: they are induced by the wind but in fact represent the effect of geostrophic adjustment over much longer time scales [*Crépon et al.*, 1989]; for this reason in the area downwind the Strait of Bonifacio, i.e., in the Tyrrhenian zone where winds are generally the most intense, the MKE relative difference shows only a marginal maximum. On the contrary, maxima of this difference are found in correspondence of subareas of the southern part of the basin, where the mean surface velocity field is much weaker and more subject to the short-term wind effect.

[46] In order to better check on the consistency between the Lagrangian measurements and the altimeter data set, and to evaluate how much of the observed differences can be related to dynamical processes, the pseudo-Eulerian statistics derived from the drifters have also been spatially smoothed. The data have been smoothed using a moving average with a square boxcar. The dimension of the boxcar has been chosen to be as comparable as possible to the scales of spatial decorrelation used in the optimal interpolation of altimeter data (~100 Km). The resulting fields are shown in Figures 6c and 6d.

[47] The smoothing does not modify significantly the average of the MKE and of the EKE (73 cm^2/s^2 and 66 cm2/s^2 respectively). On the western side of the basin (west of 12°E), the smoothed drifter data (Figure 6c) display approximately the same qualitative (spatial distribution of local energy minima and maxima) and quantitative (actual MKE values) patterns shown by the altimeter data of Figure 7a. This agreement is evident for the eastern side of NTC, in which the highest value of energy (~170 cm^2/s^2) characterizes the current along the Italian coast; the same values of MKE are observable in the Corsica Channel. Nevertheless, the westward flow just above 41°N observed in the altimeter data is not visible in the smoothed drifter field. On the eastern side of the Tyrrhenian Sea the value are still quite different. This is probably due to the fact that in the western area of the basin the circulation is characterized by subbasin-scale structures, while in the eastern region the circulation is more irregular and dominated by the mesoscale field. So the differences can be due to the different capacity of the instruments to sample the mesoscale dynamics.

[48] The values of the smoothed EKE estimated from the drifter data set are also in this case larger than the altimeter EKE ones, in fact the relative difference between altimeter and smoothed maps is of the order of 43%. The correlation between altimeter and drifters EKE maps and between altimeter and smoothed drifters maps is very similar (of the order of 0.37, we computed the Pearson correlation coefficient estimating its confidence levels with the Student T test). Finally, to further investigate if the differences between altimeter and drifters are due to different sampling capability and/or to dynamics, the pseudo-Eulerian statistics have been estimated from altimeter data resampled along drifter trajectories (Figures 7c and 7d).

[49] The MKE map of altimeter data sampled over drifters is quite similar to the drifters MKE maps, the value of the mean MKE is comparable to the mean MKE of drifters data (88 cm^2/s^2 and 84 cm^2/s^2 respectively); moreover the correlation between the two patterns is of the order to 0.7 with a significance of 99%. This value of correlation is very different from the correlations that we have calculated between all combinations of previous MKE maps (altimeter-drifters and altimeter-smoothed maps), that never exceeded 0.4.

[50] On the opposite, the levels of resampled altimeter EKE, the size and the orientation of the variance ellipses are still very different. The average altimeter EKE is still very low (29 cm^2/s^2) with respect to the EKE computed from the drifters, moreover the variance ellipses are more regular and smaller than those from both smoothed data and drifters. On the other hand, the correlation for the EKE maps is 0.45 with a significance of 99%.

[51] Even though the differences observed can still be partly imputed to the different intrinsic space-time sampling capability of the two instruments (drifters are smoothed spatially but not temporally, while altimeter data, though representative of a particular day, are obtained interpolating data collected at different times, that are then smoothed through statistical interpolation), the above analysis indicates that a significant part of the drifters EKE is possibly associated with ageostrophic signals. In any case, however, our results suggest that any research involving interpolated altimeter data (as modeling validations, for example) should carefully take into account that altimeter data may be biased in terms of energy involved in the variable processes.

5. Seasonal Variability

[52] In order to characterize the main seasonal variability of the circulation in the Tyrrhenian, the mean flow, MKE and EKE were computed from the four year altimeter data set separately for winter (from November to April) and summer seasons (from May to October). These two extended seasons were defined by subdividing the year in all possible couples of 6 month periods and selecting the two periods showing the maximum difference between each other. The resulting definition turned out to coincide with the choice made for the Tyrrhenian Sea by *Marullo et al.* [1994] and for the central Mediterranean by *Poulain and Zambianchi* [2007].

[53] The analysis shows (Figure 8) that the NTC is stronger in summer than in winter. From May to October it extends over the entire width of the basin, velocities and MKE levels much higher than in winter (reaching values above 200 cm^2/s^2) characterize the southern section of the cyclone. In contrast, from November to April, the NTC is confined between 10°E–11°E and 41.5°N–42.5°N, while a strong and wide northward current is observed along the Italian peninsula at the same latitudes. This current is not clearly visible in summer, when the inflow of the AW at 12.5°E appears weaker and mainly captured by the STA and by the eddy centered at 40.25°N–14°E.

[54] The structure and intensity of the NTA are linked to that of the NTC. In summer, when the NTC has an elongated shape around 41.5°N, the NTA has a zonally oriented ellipsoidal shape and it is more intense. In this period, sea

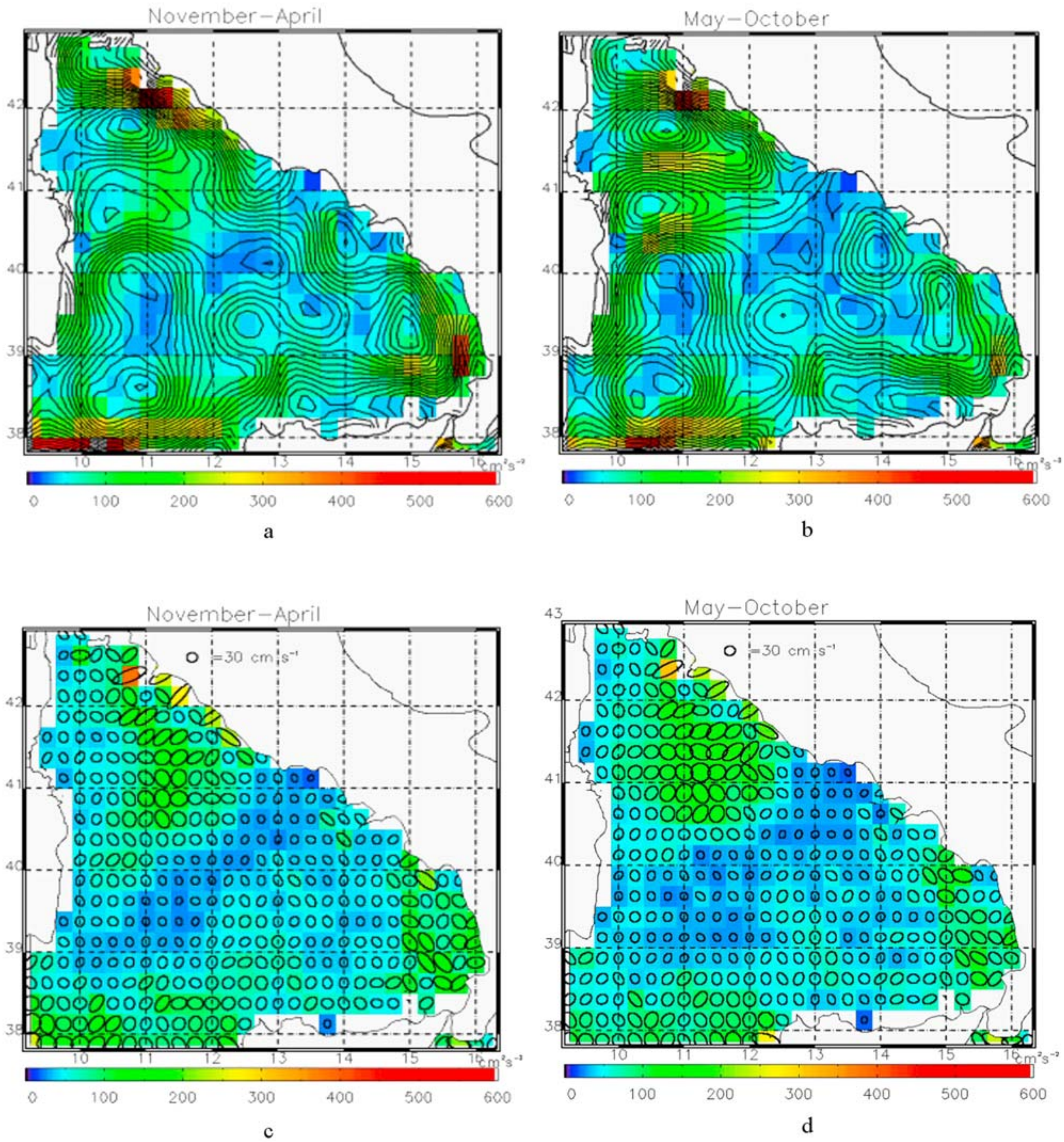

Figure 8. Seasonal variability of the Tyrrhenian Sea circulation from altimeter data. Mean kinetic energy with superimposed the mean flow vectors in (a) winter and (b) summer. Eddy kinetic energy with superimposed the variance ellipses relative in (c) winter and (d) summer.

surface heights display a strong gradient and the MKE levels reach the value of 250 cm^2/s^2. On the contrary, during winter, the NTA takes a circular form and presents MKE values of around 100 cm^2/s^2 only along its eastern and southern boundaries. The seasonal variability of the EKE is coherent with the pattern and position of these two structures. A large area of high variability occupies the entire region north of 45.5N and reaches value of the order 180 cm^2/s^2 while in winter the maximum of EKE (130 cm^2/s^2) is positioned in correspondence to the eastern boundary of the NTC and NTA.

[55] The two-core cyclonic structures present along the southeastern coast of Sardinia and elongating southward in the Sardinia channel (located in the area 10°–12°E, 38°–40°N) have the same variability of the two gyres in the north. In summer, it is characterized by higher values of MKE and the cyclonic eddy in the south of Sardinia is more intense. In the entire region off of Sardinia, Figure 8 shows

similar pattern of the variance ellipses and similar values of EKE in both winter and summer indicating that the EKE seasonal signal is very limited.

[56] On the contrary, the flow features in the southern Tyrrhenian are weaker in summer than in winter. While the shape and position of the STA and of the eddies centered at 40.25°N–14°E and 15°E–39.5°N are unchanged from one season to the other, from November to April, they display higher values of MKE and stronger gradient of sea surface heights. The EKE shows a very similar pattern in both seasons even if higher values are observed in winter, probably due to the intensification of the AW inflow.

[57] Even though the analysis on altimeter data was performed over only 4 years and the drifter trajectories are relatively sparse, the seasonality shown in the north Tyrrhenian by remote sensing and drifter data is in good agreement with former analyses [*Marullo et al.*, 1994; *Vignudelli et al.*, 1999, 2000], which leads us to believe that the Tyrrhenian indeed has a strong seasonal variability. This analysis also revealed that the seasonal signal mainly affects the mean pattern of the circulation instead of modulating its variable eddy field.

6. Conclusions

[58] The study of the Tyrrhenian surface and near surface circulation was performed analyzing 53 CODE drifters and 4 years of altimetric data. The analysis of individual drifter trajectories together with pseudo-Eulerian statistics calculated using both data sets has provided a new insight about the Tyrrhenian Sea mean surface circulation and associated variability.

[59] The circulation pattern resulting from this study is very different from that described in the literature, and new structures of the circulation are identified. In contrast to the classical view of circulation, the trajectory analysis and the pseudo-Eulerian statistics describe a circulation which only in a very broad sense can be considered as "overall cyclonic," modulated by a series of mesoscale/subbasin structures, of both transient and semipermanent nature. The importance of these structures overcomes by far the mean flow pictures, especially in the southern subbasin.

[60] Among these structures, besides the already known NTC and NTA, new structures of the circulation have been identified, specially in the southern region of the basin.

[61] In particular, between 12°E–13°E and 39°N–40°N, an anticyclone gyre (STA) has been observed in both data set as a persistent feature of the circulation. Moreover, in the southeastern region of the basin the incoming flow is deviated offshore from the Sicilian coastline by the presence of an anticyclonic gyre and it is trapped by a second cyclonic gyre located in front of the Calabrian coast. Finally, our analysis shows that the bifurcation of the AW at the southern entrance of the basin is due to the presence of the double core cyclonic structure described in section 3.3.

[62] A certain degree of seasonal variability was detected in the altimeter data. In particular, the circulation features in the western side of the basin appear to be stronger in summer than in winter. In contrast, the STA and the circulation in the southeastern region are more intense in winter than in summer. This seasonal signal affects the general pattern of the flow and the associated MKE instead of the eddy field, which is less variable with the season almost in all the basin, with the exceptions of the area occupied by the NTC and the region offshore the southeastern boundary, where higher differences are found.

[63] This observed seasonal signal seems more strongly influenced by the inflow and outflow at the main open boundary of the basin, than by the local variability of the wind field. The maximum MKE in the southern part of the basin is in phase with the outflow at the Corsica channel, consistently with *Astraldi and Gasparini*'s [1994] hypothesis that the intensification of the Tyrrhenian Sea western current is ruled by the winter surface buoyancy fluxes in the Ligurian-Provencial basin. This process also requires the increase of the inflow at the southern entrance of the basin, as visible in Figure 8, in order to compensate the increasing of outflow. This hypothesis has also been confirmed by modeling studies of the Mediterranean Sea by *Artale et al.* [2002]. Moreover, the winter increase of the Tyrrhenian outflow is known to be responsible to the NTC dislocation toward Corsica and its meridional orientation. Since the NTC-NTA system is driven by the wind stress curl at Strait of Bonifacio, observed all year-round [*Artale et al.*, 1994], it is not surprising that these features are always present in our data. The apparent contradictory seasonal maximum EKE in the summer season when northwestern winds are less intense with respect to the winter season can be attributed to the same process. In summer, when the outflow is minimum, the basin can respond to local forcing and internal dynamics, and the variability of the wind stress at the Strait of Bonifacio can drive a higher variability in the strength and position of the NTC, as observed also in the infrared imagery by *Marullo et al.* [1994] and *Perilli et al.* [1995].

[64] The pseudo-Eulerian statistics computed with the two data sets highlighted the sampling and dynamical differences between drifter and altimeter measurements. The MKE levels of energy are quite similar when comparing the altimeter data sampled over drifter trajectories with the spatially smoothed pseudo-Eulerian statistics derived from drifter. However, the variance ellipses and the EKE levels computed from altimeter measurements are always smaller than those from drifters. Consequently, we may conclude that, even though altimeter data obviously ensure a wider and more regular sampling, they are missing a considerable part of the signal, at least when considering the standard interpolated products.

[65] **Acknowledgments.** The Lagrangian experiment was organized in the framework of the "Programma Ambiente Mediterraneo" initiative, funded by the Italian Ministry for Research through ENEA (subproject 3.3.2.3 on drifting buoy analysis, whose coordinator is Volfango Rupolo, whom we thank for fruitful cooperation) with additional funding obtained from the U.S. Office of Naval Research. The ISAC work was partially supported by European Commission under contracts N036949 and N218812. P.M.P. was partially supported by the Office of Naval Research under grants N0001499WR30014, N0001400WR20193, and N0001401WR20147. Data quality control, preprocessing, and interpolation was carried out by Laura Ursella at OGS, whose help is gratefully acknowledged. Preliminary work on the drifter data was done by Pierpaolo Falco (who took care of most deployments), Santa Paola Fico, Valentina Lignitto, Milena Menna, and Marilisa Trani. The authors acknowledge insightful discussions with Francesco Bignami. Moreover, we are grateful to the reviewers for their suggestions and comments on the earlier version of this work, which helped to improve the manuscript.

References

Aliverti, G., M. Picotti, L. Trotti, A. De Maio, O. Lauretta, and M. Moretti (1968), *Atlante del Mar Tirreno: Isoterme ed isoaline Dedotte Dalle Misure Delle Crociere per l'Anno Geofisico Internazionale 1957–1958*, 127 pp., Tipografia Genovese, Naples, Italy.

Artale, V., M. Astraldi, G. Buffoni, and G. P. Gasparini (1994), Seasonal variability of the gyre-scale circulation in the nor northern Tyrrhenian Sea, *J. Geophys. Res.*, *99*, 14,127–14,137, doi:10.1029/94JC00284.

Artale, V., D. Iudicone, R. Santoleri, V. Rupolo, S. Marullo, and F. D'Ortenzio (2002), The role of surface fluxes in OGCM using satellite SST: Validation of and sensitivity to the forcing frequency of the Mediterranean thermohaline circulation, *J. Geophys. Res.*, *107*(C8), 3120, doi:10.1029/2000JC000452.

Astraldi, M., and G. P. Gasparini (1994), The seasonal characteristics of the circulation in the Tyrrhenian sea, in *Seasonal and Interannual Variability of the Western Mediterranean Sea*, *Coastal Estuarine Stud. Ser.*, vol. 46, edited by P. E. La Violette, pp. 115–134, AGU, Washington, D. C.

Astraldi, M., G. P. Gasparini, A. Vetrano, and S. Vignudelli (2002), Hydrographic characteristics and interannual variability of water masses in the central Mediterranean: A sensitivity test for long-term changes in the Mediterranean Sea, *Deep Sea Res. Part I*, *49*(4), 661–680, doi:10.1016/S0967-0637(01)00059-0.

Bauer, S., M. S. Swenson, A. Griffa, A. J. Mariano, and K. Owens (1998), Eddy-mean flow decomposition and eddy-diffusivity estimates in the Tropical Pacific Ocean: 1. Methodology, *J. Geophys. Res.*, *103*, 30,855–30,871, doi:10.1029/1998JC900009.

Bentivegna, F., F. Valentino, P. Falco, E. Zambianchi, and S. Hochscheid (2007), The relationship between loggerhead turtle (Caretta caretta) movement patterns and Mediterranean currents, *Mar. Biol. Berlin*, *151*, 1605–1614, doi:10.1007/s00227-006-0600-1.

Buongiorno Nardelli, B., G. Larnicol, E. D'Acunzo, R. Santoleri, S. Marullo, and P. Y. Le Traon (2002), Near real time SLA and SST products during 2-years of MFS pilot project: Processing, analysis of the variability and of the coupled patterns, *Ann. Geophys.*, *20*, 1–19.

Crépon, M., M. Boukthir, M. Barnier, and F. Aikman III (1989), Horizontal ocean circulation forced by deep water formation. Part I: An analytical study, *J. Phys. Oceanogr.*, *19*, 1781–1792, doi:10.1175/1520-0485(1989)019<1781:HOCFBD>2.0.CO;2.

Davis, R. E. (1985), Drifter observations of coastal currents during CODE: The method and descriptive view, *J. Geophys. Res.*, *90*, 4741–4755, doi:10.1029/JC090iC03p04741.

Ducet, N., P. Y. Le Traon, and G. Reverdin (2000), Global high-resolution mapping of ocean circulation from TOPEX/Poseidon and ERS-1 and -2, *J. Geophys. Res.*, *105*(C8), 19,477–19,498, doi:10.1029/2000JC900063.

Elliot, A. J., and F. De Strobel (1978), Oceanographic conditions in the coastal waters of N.W. Italy during the spring of 1977, *Bol. Geofis. Teor. Appl.*, *79*, 251–262.

Emery, W. J., and R. E. Thomson (1998), *Data Analysis Methods in Physical Oceanography*, Pergamon, Oxford, U. K.

Gasparini, G. P., G. Zodiatis, M. Astraldi, C. Galli, and S. Sparnocchia (1999), Intermediate water lenses in the Ligurian Sea, *J. Mar. Syst.*, *20*, 319–332, doi:10.1016/S0924-7963(98)00089-X.

Iudicone, D., R. Santoleri, S. Marullo, and P. Gerosa (1998), Sea level variability and surface eddy statistices in the Mediterranean Sea from TOPEX/POSEIDON data, *J. Geophys. Res.*, *103*(C2), 2995–3011, doi:10.1029/97JC01577.

Krivosheya, V. G., and I. M. Ovchinnikov (1973), Pecularities in the geostrophic circulation of the waters of the Tyrrhenian Sea, *Oceanology Engl. Transl.*, *13*, 822–827.

Larnicol, G., N. Ayoub, and P. Y. Le Traon (2002), Major changes in Mediterranean Sea level variability from 7 years of TOPEX/Poseidon and ERS-1/2 data, *J. Mar. Syst.*, *33–34*, 63–89, doi:10.1016/S0924-7963(02)00053-2.

Malanotte-Rizzoli, P., et al. (1999), The eastern Mediterranean in the 80s and in the 90s: The big transition in the intermediate and deep circulations, *Dyn. Atmos. Oceans*, *29*, 365–395, doi:10.1016/S0377-0265(99)00011-1.

Marullo, S., R. Santoleri, and F. Bignami (1994), The surface characteristics of the Tyrrhenian sea: Historical satellite data analysis, in *Seasonal and Interannual Variability of the Western Mediterranean Sea*, *Coastal Estuarine Stud. Ser.*, vol. 46, edited by P. E. La Violette, pp. 135–154, AGU, Washington, D. C.

Mauri, E., and P.-M. Poulain (2004), Wind-driven currents in Mediterranean drifter-data, *Tech. Rep. 01/2004/OGA/1*, 25 pp., Oceanogr. Geofis. Sper., Trieste, Italy.

Millot, C. (1987), Circulation in the western Mediterranean, *Oceanol. Acta*, *10*(2), 143–149.

Millot, C. (1999), Circulation in the western Mediterranean Sea, *J. Mar. Syst.*, *20*, 423–442, doi:10.1016/S0924-7963(98)00078-5.

Nielsen, J. N. (1912), Hydrography of the Mediterranean and adjacent waters, *Rep. Dan. Oceanogr. Exp. 1908–1910 Medit. Adjacent Waters*, *1*, 72–191.

Perilli, A., V. Rupolo, and E. Salusti (1995), Satellite investigations of a cyclonic gyre in the central Tyrrhenian Sea (western Mediterranean Sea), *J. Geophys. Res.*, *100*, 2487–2500, doi:10.1029/94JC01315.

Poulain, P.-M. (2001), Adriatic Sea Surface Circulation as derived from drifter data between 1990 and 1999, *J. Mar. Syst.*, *29*, 3–32, doi:10.1016/S0924-7963(01)00007-0.

Poulain, P.-M., and E. Zambianchi (2007), Near-surface circulation in the central Mediterranean Sea as deduced from Lagrangian drifters in the 1990s, *Cont. Shelf Res.*, *27*(7), 981–1001, doi:10.1016/j.csr.2007.01.005.

Poulain, P.-M., R. Barbanti, R. Cecco, C. Fayos, E. Mauri, L. Ursella, and P. Zanasca (2004), Mediterranean Surface Drifter Database: 2 June 1986 to 11 November 1999, *Tech. Rep. 78/2004/OGA/31*, Oceanogr. Geofis. Sper., Trieste, Italy.

Poulain, P.-M., et al. (2007), MedArgo: A drifting profiler program in the Mediterranean Sea, *Ocean Sci.*, *3*, 379–395.

Poulain, P.-M., R. Gerin, E. Mauri, and R. Pennel (2009), Wind effects on drogued and undrogued drifters in the eastern Mediterranean, *J. Atmos. Oceanic Technol.*, *26*, 1144–1156, doi:10.1175/2008JTECHO618.1.

Pujol, M.-I., and G. Larnicol (2005), Mediterranean sea eddy kinetic energy variability from 11 years of altimetric data, *J. Mar. Syst.*, *58*, 121–142, doi:10.1016/j.jmarsys.2005.07.005.

Ralph, E. A., and P. P. Niiler (1999), Wind driven currents in the tropical Pacific, *J. Phys. Oceanogr.*, *29*, 2121–2129, doi:10.1175/1520-0485(1999)029<2121:WDCITT>2.0.CO;2.

Rio, M.-H., and F. Hernandez (2004), A mean dynamic topography computed over the world ocean from altimetry, in-situ measurements and a geoid model, *J. Geophys. Res.*, *109*, C12032, doi:10.1029/2003JC002226.

Rio, M.-H., P.-M. Poulain, A. Pasqual, E. Mauri, G. Larnicol, and L. Santoleri (2007), A mean dynamic topography of the Mediterranean Sea computer from the altimetric data and in situ measurements, *J. Mar. Syst.*, *65*, 484–508, doi:10.1016/j.jmarsys.2005.02.006.

Robinson, A. R., W. G. Leslie, A. Theocharis, and A. Lascaratos (2001), Mediterranean Sea circulation, in *Encyclopedia of Ocean Sciences*, edited by J. H. Steele, K. K. Turekian, and S. A. Thorpe, pp. 1689–1705, Academic, London.

Sparnocchia, S., G. P. Gasparini, M. Astraldi, M. Borghini, and P. Pistek (1999), Dynamics and mixing of the eastern Mediterranean outflow in the Tyrrhenian Basin, *J. Mar. Syst.*, *20*, 301–317, doi:10.1016/S0924-7963(98)00088-8.

Swenson, M. S., and P. P. Niiler (1996), Statistical analysis of the surface circulation of the California Current, *J. Geophys. Res.*, *101*, 22,631–22,645, doi:10.1029/96JC02008.

Tait, R. T. (1984), The physical oceanography of the Tyrrhenian and Ligurian Sea, paper presented at 6th Congresso, Assoc. Ital. di Oceanol. e Limnol., Leghorn, Italy.

Vignudelli, S., G. P. Gasparini, M. E. Schiano, and M. Astraldi (1999), A possible influence of the North Atlantic Oscillation on the western Mediterranean circulation, *Geophys. Res. Lett.*, *26*, 623–626, doi:10.1029/1999GL900038.

Vignudelli, S., P. Cipollini, M. Astraldi, G. P. Gasparini, and G. M. R. Manzella (2000), Integrated use of altimeter and in situ data for understanding the water exchanges between the Tyrrhenian and Ligurian seas, *J. Geophys. Res.*, *105*, 19,649–19,663, doi:10.1029/2000JC900083.

B. Buongiorno Nardelli, E. Rinaldi, and R. Santoleri, Istituto di Scienze dell'Atmosfera e del Clima, CNR, Via Fosso del Cavaliere 100, I-00133 Rome, Italy. (eleonora.rinaldi@artov.isac.cnr.it)

P.-M. Poulain, Dipartimento di Oceanografia, Istituto Nazionale di Oceanografia e di Geofisica Sperimentale, Borgo Grotta Gigante 42/c, I-34010 Trieste, Italy.

E. Zambianchi, Dipartimento di Scienze per l'Ambiente, Università degli Studi di Napoli "Parthenope," Centro Direzionale di Napoli, Isola C4, I-80143 Naples, Italy.